Tethered Polymer-Supported Planar Lipid Bilayers for Reconstitution of Integral Membrane Proteins: Silane-Polyethyleneglycol-Lipid as a Cushion and Covalent Linker

Michael L. Wagner and Lukas K. Tamm
Department of Molecular Physiology and Biological Physics, University of Virginia, Charlottesville, Virginia 22908-0736 USA

ABSTRACT There is increasing interest in supported membranes as models of biological membranes and as a physiological matrix for studying the structure and function of membrane proteins and receptors. A common problem of protein-lipid bilayers that are directly supported on a hydrophilic substrate is nonphysiological interactions of integral membrane proteins with the solid support to the extent that they will not diffuse in the plane of the membrane. To alleviate some of these problems we have developed a new tethered polymer-supported planar lipid bilayer system, which permitted us to reconstitute integral membrane proteins in a laterally mobile form. We have supported lipid bilayers on a newly designed polyethyleneglycol cushion, which provided a soft support and, for increased stability, covalent linkage of the membranes to the supporting quartz or glass substrates. The formation and morphology of the bilayers were followed by total internal reflection and epifluorescence microscopy, and the lateral diffusion of the lipids and proteins in the bilayer was monitored by fluorescence recovery after photobleaching. Uniform bilayers with high lateral lipid diffusion coefficients ($0.8–1.2 \times 10^{-8}$ cm^2/s) were observed when the polymer concentration was kept slightly below the mushroom-to-brush transition. Cytochrome b_5 and annexin V were used as first test proteins in this system. When reconstituted in supported bilayers that were directly supported on quartz, both proteins were largely immobile with mobile fractions $< 25\%$. However, two populations of laterally mobile proteins were observed in the polymer-supported bilayers. Approximately 25% of cytochrome b_5 diffused with a diffusion coefficient of $\sim 1 \times 10^{-8}$ cm^2/s, and 50–60% diffused with a diffusion coefficient of $\sim 2 \times 10^{-10}$ cm^2/s. Similarly, one-third of annexin V diffused with a diffusion coefficient of $\sim 3 \times 10^{-9}$ cm^2/s, and two-thirds diffused with a diffusion coefficient of $\sim 4 \times 10^{-10}$ cm^2/s. A model for the interaction of these proteins with the underlying polymer is discussed.

INTRODUCTION

Since their inception (Tamm and McConnell, 1985), supported lipid bilayers have been widely used as models for cellular membranes (McConnell et al., 1986; Sackmann, 1996). Supported membranes, monolayers and bilayers, have been used in fundamental and applied studies of lipid assembly on surfaces (Kalb et al., 1992; Wenzl et al., 1994; Hubbard et al., 1998), membrane structure (Tamm and Shao, 1998), membrane dynamics (Tamm and Kalb, 1993; Thompson et al., 1993), lipid-protein interactions (Tamm and Tatulian, 1997; Silvestro and Axelsen, 1998), ligand-receptor interactions (Thompson et al., 1997; Heyse et al., 1998), electrochemical properties of membranes (Stelzle et al., 1993; Fromherz et al., 1999), the development of membrane-based biosensors (Cornell et al., 1997; Stora et al. 1999), and microscopic separation devices (van Oudenaarden and Boxer, 1999). Although supported bilayers and, to a more limited extent, supported monolayers were used so successfully to study properties of peripheral membrane proteins, membrane-integrated peptides, and the binding of fluorescent ligands to integral membrane protein receptors, they have one serious limitation: bilayers that are directly supported on glass or quartz are separated from the substrate by a thin (10–20 Å), lubricating film of water (Tamm and McConnell, 1985; Johnson et al., 1991). This film is sufficient to support the lateral mobility of lipids in both leaflets of the bilayer (Tamm, 1988), but the substrate-exposed domains of large integral membrane proteins interact with the hydrophilic substrate to the extent that they pin these proteins to the substrate and thereby inhibit their lateral mobility (Poglitsch et al., 1991; Hinterdorfer et al., 1994; Salafsky et al., 1996).

Many reactions in membranes depend on lateral motion and the fluid dynamic properties of all membrane components. Therefore, an important goal for the further development of supported membranes as surrogate cell membranes must be to fully reproduce the lateral mobility of all membrane components, including transmembrane proteins in these systems. Several attempts to achieve this goal have been made in recent years. The general approach of these studies was to separate the membrane from the solid support with a polymer cushion (see, e.g., Sackmann, 1996). However, most of these efforts have met with only limited success. Often the bilayers that were formed on polymers were patchy and exhibited lots of defects, and reconstitution of integral membrane proteins and lateral diffusion measurements of these proteins (i.e., the really critical test for improvement over the existing systems) has rarely been attempted. In an early study, Spinke et al. (1992) self-assembled a moderately hydrophilic, methacrylic coblock

Received for publication 13 December 1999 and in final form 13 June 2000.

Address reprint requests to Dr. Lukas K. Tamm, Department of Molecular Physiology and Biological Physics, University of Virginia, P. O. Box 800736, Charlottesville, VA 22908-0736. Tel.: 804-982-3578; Fax: 804-982-1616; E-mail: lkt2e@virginia.edu.

© 2000 by the Biophysical Society

0006-3495/00/09/1400/15 $2.00

polymer with aliphatic side chains on a gold surface. The subsequent fusion of lipid vesicles to this surface was followed with surface plasmon spectroscopy. The resulting lipid bilayers were not further characterized. Kühner et al. (1994) prepared 30–40-μm-thick polyacrylamide gels on glass and coated these with monolayers and bilayers, using Langmuir-Blodgett techniques. When inspected by epifluorescence microscopy, these bilayers exhibited some residual domain structure. Lipids and a lipid-linked 20-residue peptide antigen diffused normally in these bilayers. In an extension of this work, the electrophoretic mobility of charged lipids was determined in monolayers that were supported on agarose gels (Dietrich and Tampé, 1995). Bilayers were not formed on these substrates. In another study, bilayers were formed on a polyvinyl substrate that had functionalized diethylene amino groups for reaction with lipid headgroups (Beyer et al., 1996). Although homogeneous bilayers with high lipid diffusion coefficients were obtained under some conditions, the hydrophilic linkers are clearly too short to accommodate membrane proteins in this system. Unreacted positively charged ammonium groups may also pose a problem for the functional reconstitution of membrane proteins. The same charge problem exists for bilayers that are supported on a cushion of polyethyleneimine (Majewski et al., 1998b; Wong et al., 1999a,b). Wong et al. (1999a) characterized lipid bilayers that were supported on a polyethyleneimine cushion by neutron reflectometry and found that the thickness, surface roughness, and coverage of the polymer and lipid layers depended strongly on the method of preparation. For example, the polymer was ~170 Å thick when the bilayers were adsorbed to the quasi-dried preadsorbed polymer, but only 40–50 Å thick when the polymer was added after deposition of the lipid bilayer. Elender et al. (1996) were able to produce uniformly fluorescent bilayers of dimyristoylphosphatidylcholine and 20 mol% cholesterol on 600–800-nm cushions of dextran. The lateral diffusion coefficient and mobile fraction of the lipids were high in this system, which, however, was very unstable in the absence of cholesterol.

A successful polymer for the support of protein-containing lipid bilayers must fulfill the following requirements: it should be very hydrophilic and should interact neither with membrane lipids nor with membrane proteins; for robustness in practical applications, it should also be chemically linked to the bilayer at one end and to the solid substrate (quartz or glass) at the other end and should not engage in extensive physical interactions with either surface. Polyethyleneglycol (PEG), covalently linked to the substrate and the bilayers, is likely to fulfill these criteria. PEG is known to prevent the nonspecific adsorption of proteins to surfaces (Prime and Whitsides, 1991; Jin et al., 1995; Du et al., 1997). For this reason it has been extensively used to coat the surfaces of biomedical devices. Moreover, PEG does not adsorb to lipid bilayer surfaces (Arnold et al., 1990) and shields liposomes from unwanted interactions with biomaterials in drug delivery systems (Woodle and Lasic, 1992). Similarly, we expect that PEG interacts only minimally with glass or quartz surfaces. For example, soluble PEG cannot be transferred from the subphase under a compressed lipid monolayer (Ariga et al., 1995). Based on these favorable observations, we designed a new PEG-phospholipid conjugate that could be covalently bonded to silicate substrates. In this paper, we describe the design and use of this molecule to form tethered polymer-supported lipid bilayers. We further describe the reconstitution and lateral diffusion experiments of two proteins that represent two different structural classes of membrane proteins. Conditions are explored that produce uniformly fluorescent tethered polymer-supported bilayers with high lateral mobilities of the constituent lipids and proteins.

MATERIALS AND METHODS

Materials

1-Palmitoyl-2-oleoyl-*sn*-glycero-3-phosphocholine (POPC), 1-palmitoyl-2-oleoyl-*sn*-glycero-3-[phospho-*rac*-(1-glycerol)] (POPG), 1,2-dioleoyl-*sn*-glycero-3-phosphocholine (DOPC), and *N*-[poly(ethylene glycol) 2000]-1,2-dimyristoyl-*sn*-glycero-3-phosphoethanolamine (PEG2000-DMPE) were purchased from Avanti Polar Lipids (Alabaster, AL). *N*-(7-Nitrobenz-2-oxa-1,3-diazol-4-yl)-egg phosphoethanolamine (NBD-eggPE) and fluorescein-5-isothiocyanate (FITC) were from Molecular Probes (Eugene, OR), and β-octyl-glucoside (β-OG) was from Sigma (St. Louis, MO). Quartz slides (37 mm × 25 mm × 1 mm) were purchased from Quartz Scientific (Fairport Harbor, OH). DMPE-PEG-triethoxysilane (DPS) was custom-synthesized by Shearwater Polymers (Huntsville, AL). ^{1}H-NMR spectra of DPS in DMSO-d_6 confirmed the correct structure of this molecule. Rabbit cytochrome b_5 was expressed in *Escherichia coli* and was purified as previously described (Ladokhin et al., 1991), and was a gift from Dr. Peter Holloway (University of Virginia, Charlottesville, VA). Human recombinant fluorescein-labeled annexin V was purchased from Alexis Biochemicals (San Diego, CA) and used as received.

Substrates and monolayers

Quartz and glass microscope slides were cleaned by first boiling in a 10% solution of Contrad 70 (Fisher Scientific, Pittsburgh, PA) and sonicating hot in detergent for 10 min, followed by extensive rinsing with double-distilled water and high-purity methanol. The slides were then dried in an oven at 70°C and stored in a dust-free container until use. Immediately before use, the slides were further cleaned in an argon plasma cleaner (Harrick Scientific Corp., New York) at high setting for 10 min.

Lipid monolayers were spread from 10 mM solutions of lipid in hexane/ethanol (9:1) or chloroform (monolayers containing PEG lipids) at near-zero surface pressure at the air-water interface of a Langmuir-Blodgett trough (model 611; Nima Technologies, Coventry, England). The subphase was 10 mM Tris-acetic acid (pH 5.0) made from double-distilled water. Solvents were allowed to evaporate for 20 min before the monolayers were compressed. A compression rate of 25 cm^2/min was used to record surface pressure-area isotherms. Monolayers were transferred to quartz microscope slides at a pressure of 32 mN/m. This was accomplished by first forming a monolayer at ~0 pressure and compressing it to 32 mN/m. The plasma cleaned slides were quickly (200 mm/min) immersed through the monolayer and into the trough. No lipid was transferred at this step, as the surface pressure was virtually unchanged. The slides were withdrawn from the subphase at a rate of 5 mm/min while a surface pressure of 32 mN/m

was maintained with an electronic feedback circuit. A single monolayer was formed in this step on the surface, as verified by the ~1:1 transfer ratio. When required, we tethered the DPS molecules to the surface by drying the coated slides in a desiccator at room temperature overnight and subsequently curing them in a 70°C oven for 40 min. The hot slides were transferred to a desiccator, allowed to equilibrate at room temperature, and typically used on the same day.

X-ray photoelectron spectroscopy

X-ray photoelectron spectroscopy (XPS) spectra of supported monolayers and pure quartz surfaces were recorded on a PHI 560 ESCA/sam system (Perkin-Elmer, Norwalk, CT), using Mg $K\alpha_{1,2}$ as an x-ray source. The resolution was 1 eV in the full-range scans and 0.2 eV in the scans examining the substructure of the C_{1s} peak. Samples of DPS or PEG2000-DMPE were prepared and cured as described above. The surfaces were then thoroughly rinsed with methanol to remove all lipids that were not covalently bound to the surface. Gaussian components of the C_{1s} peak were fitted using IGOR software (Wavemetrics, Portland, OR).

Large unilamellar vesicles

Lipids were mixed in appropriate proportions from stock solutions in chloroform, dried on the bottom of glass test tubes by a stream of nitrogen, desiccated under vacuum for 1 h, and hydrated by the addition of HEPES buffer (5 mM HEPES, pH 7.4, containing 150 mM NaCl) to give the desired lipid concentration. Resulting lipid suspensions were vigorously vortexed, freeze-thawed five times, and extruded nine times through two polycarbonate membranes of 100-nm pore size, using a syringe-type extruder (Avestin, Ottawa, ON, Canada).

Supported bilayers

Dry supported monolayers (with or without polymer, cured or uncured) were assembled in a closed home-built total internal reflection fluorescence microscopy (TIRFM) measuring cell (Tamm, 1993). Supported bilayers were formed by the addition of 1.1 ml of 100 μM lipid vesicles. Lipid vesicles are known to spread on (or fuse with) supported monolayers under these conditions (Kalb et al., 1992). The kinetics of bilayer formation were followed in many cases by TIRFM. After 2 h of equilibration at room temperature, excess unfused vesicles were flushed out of the measuring cell with 5 volumes of buffer. Epifluorescence micrographs were taken on a Zeiss Axiovert 35 microscope (Carl Zeiss, Thornwood, NY), using a 40× water immersion objective and a EG&G 512 × 512 cooled charge-coupled device camera (PARC, Princeton, NJ). The bilayers were stable for at least 24 h and sometimes much longer. Supported bilayers containing the integral membrane protein cytochrome b_5 were prepared identically, except that reconstituted proteoliposomes instead of pure lipid vesicles were used.

Total internal reflection fluorescence microscopy and fluorescence recovery after photobleaching

The laser fluorescence microscope that was used for the TIRFM and fluorescence recovery after photobleaching (FRAP) experiments has been described in detail elsewhere (Kalb et al., 1990, 1992) and is described here only briefly. For TIRFM, the beam of an argon ion laser (Innova 300-4 or Innova 300-8; Coherent, Palo Alto, CA) operating at 488 nm was focused and directed through a trapezoid quartz prism to the lower surface of a quartz slide, which forms the top of the experimental measuring cell. The beam was totally internally reflected at the quartz-buffer interface at an incident angle of 72° from the normal (the critical angle is 65°). An elliptical area, ~250 μm × 65 μm, was illuminated. Fluorescence resulting from excitation by the evanescent wave, which penetrates ~90 nm (1/e) into the adjacent buffer phase, was collected through a 40× water immersion objective on the Axiovert 35. The fixed prism was lubricated and optically coupled to the slide to allow for simple translocation of the measuring cell on the microscope stage. Fluorescence was recorded from the central section of the ellipse with a photomultiplier tube. FRAP experiments were carried out on the same samples on the same microscope by bleaching a pattern of parallel stripes, formed by imaging a Ronchi ruling into the image plane, and measuring the integrated fluorescence recovery of an ~100 μm^2 area with a photomultiplier tube (Smith and McConnell, 1978). Fluorescence recovery curves were fit to the equation

$$F(t) = F_\infty + (F_0 - F_\infty)\exp(-D_L a^2 t) \quad (1)$$

where $a = 2\pi/p$, D_L is the lateral diffusion coefficient, p is the stripe period, and F_0 and F_∞ are the fluorescence intensities immediately after and a very long time after the bleach pulse, respectively. In pattern photobleaching, the mobile fraction as a percentage is defined as

$$\text{mobile fraction} = [(F - F_0)/(F_{pre} - F_0)] \times 200 \quad (2)$$

where F_{pre} is the fluorescence intensity before the bleach pulse.

Labeling and reconstitution of cytochrome b_5

Cytochrome b_5 was labeled with fluorescein as previously described (Kalb and Tamm, 1992). Briefly, 50 μg of FITC was reacted with 1 mg of protein in 50 mM carbonate buffer (pH 9.2) containing 150 mM NaCl and 100 mM β-OG, for 2 h at room temperature. Unreacted FITC was removed by Sephadex G-25 column chromatography with Tris-OG buffer (10 mM Tris-HCl (pH 7.4), 150 mM NaCl, 100 mM β-OG). The resulting fluorescein/protein ratio was 3:1 (mol/mol) as determined by absorbance spectroscopy (a molar extinction coefficient of 73,000 at 494 nm was used for fluorescein) and the Biorad protein assay. For reconstitution into proteoliposomes, the desired concentration of cytochrome b_5 in 0.5 ml of Tris-OG buffer was added to 150 μmol of POPC that had been dried on the bottom of a test tube. After thorough mixing, the solution was dialyzed against the same buffer without detergent for 18 h with two changes of buffer. The resulting proteoliposomes were loaded onto a 10%, 30%, 45% discontinuous sucrose gradient and centrifuged for 90 min at 45,000 rpm in a SW55Ti rotor. A single fluorescent band was collected at the 0/10 interface, and the lipid/protein ratio was determined, using the Bradford protein assay and a modified Ames (1966) phosphate assay to estimate lipid concentrations.

Binding of annexin V to supported bilayers

Asymmetrical bilayers consisting of POPC with or without DPS in the inner layer and POPC:POPG (9:1) in the outer layer were prepared in an EDTA-containing buffer (10 mM HEPES, 100 mM NaCl, 1 mM EDTA, pH 7.4). To remove any excess adsorbed vesicles, the bilayers were first washed with 10 volumes of EDTA-containing buffer followed by 3 volumes of the same buffer containing 1 mM $CaCl_2$ instead of EDTA. Fluorescein-labeled annexin V (56 pmol) in 1 ml of the Ca^{2+}-containing buffer was injected into the sample cell, and the binding of annexin V was followed by TIRFM. The cell was then washed with 10 volumes of the Ca^{2+}-containing buffer to remove unbound proteins.

RESULTS

A new polymer-lipid molecule to tether lipid bilayers to hydrophilic solid substrates

Lipid bilayers that are supported on silicate substrates are typically lubricated by a thin film of water on the order of

~10 Å thick. To accommodate integral membrane proteins with hydrophilic domains on both sides of the bilayer, we designed a new polymer-lipid molecule that we expected would increase the distance between the substrate and the bilayer while still keeping the bilayer stably attached (tethered) to the solid support (Fig. 1). This molecule consists of dimyristoylphosphatidylethanolamine (DMPE), polyethyleneglycol (PEG), and a triethoxysilane group for covalent linkage to silanols at the surface of silicate substrates. The PEG moiety contains, on average, 77 subunits, and according to the manufacturer's specifications, it is fairly monodisperse. We chose PEG as the polymer because of its nearly ideal polymer behavior in water ("theta" solvent) and its negligible interactions with proteins. We call this molecule DPS.

To estimate the polymer behavior of DPS on surfaces, we first calculated according to the de Gennes theory of grafted neutral polymers the average distance between graft sites and the extension length of the polymer as a function of the mol fraction of DPS in a lipid monolayer (de Gennes, 1987). The average distance between graft sites, D, is simply given by the square root of the area, A, of a single lipid molecule (70 Å^2 for POPC and DMPE in the fluid state) and the mol fraction, f, of DPS in the membrane:

$$D = (A/f)^{1/2} \tag{3}$$

The Flory radius of a polymer of N subunits of length a is

$$R_F = a \cdot N^{3/5} \tag{4}$$

At $D > R_F$, the extension length, L, of the polymer above the surface equals R_F. The average shape of the polymer is a sphere of radius R_F. Individual mushrooms of polymer are attached to the surface at each grafting site. In this regime, the polymer is assumed to interact neither with the surface nor with its nearest neighbors. However, when $D < R_F$, the polymers will interact laterally and will extend farther from the surface. A dense polymer "brush" is formed on the surface under these conditions. Following de Gennes' scaling laws, the extension length of the polymer brush in this regime is given by

$$L = a \cdot N(a/D)^{2/3} \tag{5}$$

For our polymer of 77 units of 3.5 Å, we calculate R_F = 47.5 Å. The theoretically expected behavior of D and L as a function of the mol fraction of DPS in a monolayer is plotted in Fig. 2. According to these (idealized) calculations the mushroom-to-brush transition is predicted to occur at 3.1 mol% DPS (Fig. 2). Near this transition the polymer layer on the surface is expected to be ~48 Å thick. The cartoon of the polymer-supported bilayer in Fig. 1 *A* is drawn approximately to scale.

Pressure-area isotherms of DPS in POPC

To experimentally examine polymer interactions on membrane surfaces, the DPS molecule was included in monolayers of POPC at different mole fractions on a Langmuir

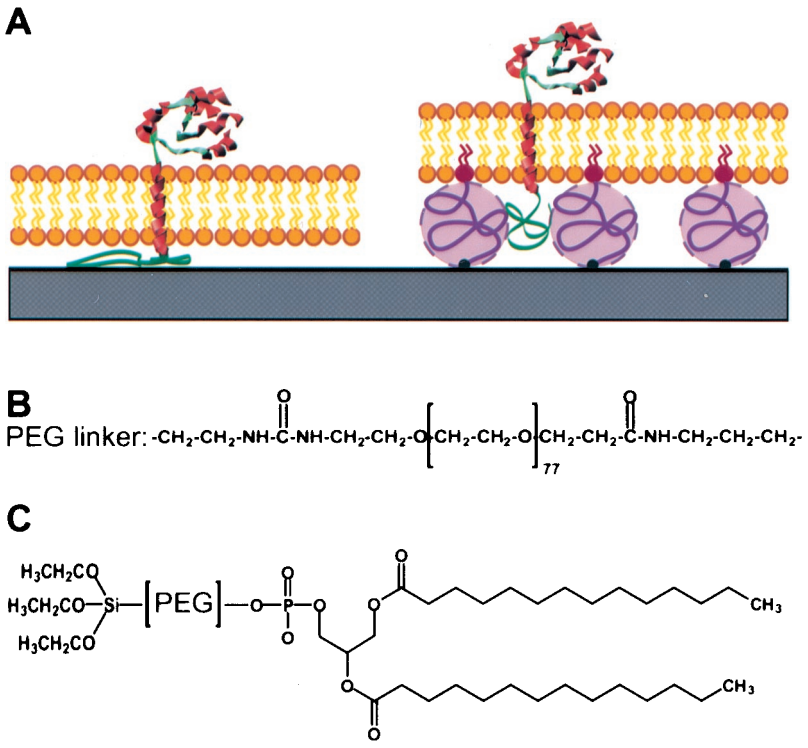

FIGURE 1 Design of a tethered polymer-supported lipid bilayer. (*A*) Polymer-supported lipid bilayers are designed to space the lipid bilayer from the supporting solid substrate to allow for the reconstitution of integral membrane proteins by minimizing interactions of the proteins with the substrate and the polymer. To make the system physically robust, the linear polymer is covalently attached at its two ends to the substrate and membrane lipids, respectively. Approximately drawn to scale. (*B*) Chemical structure of the linker between the silane and DMPE in DPS. (*C*) Structure of a lipid polymer, DPS, with a silane group for covalent tethering to silicates. PEG, polyethyleneglycol of 77 subunits.

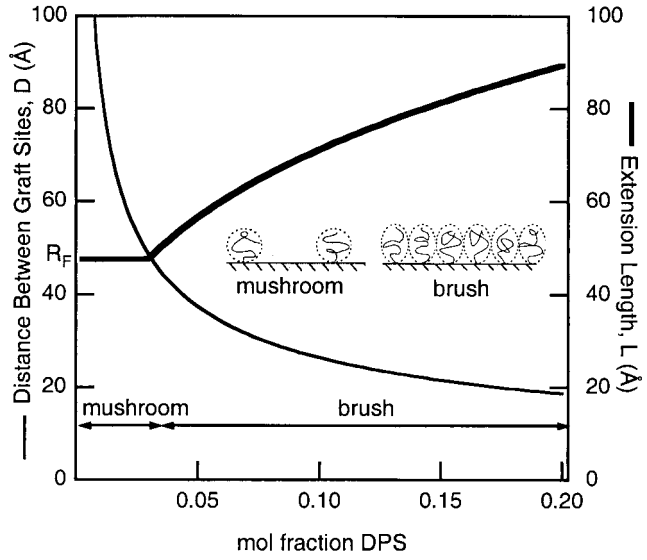

FIGURE 2 Theoretical predictions for the structural parameters of DPS on surfaces. The average distances between graft sites and extension lengths of the polymer are calculated as a function of the graft site density according to the de Gennes theory of uncharged grafted polymers on surfaces. See text for details. R_F, Flory radius. A transition from the mushroom to the brush regime is predicted to occur at 3.1 mol% DPS.

trough, and pressure-area isotherms were recorded (Fig. 3). As the mol fraction of DPS in the monolayer was increased, a large expansion of the monolayer appeared at surface pressures below 12 mN/m, indicating an increased area per molecule. Fig. 3 also shows that a transition between a liquid-expanded and a liquid-condensed phase occurs at ~12 mN/m. This transition can be observed at DPS concentrations as low as 0.5 mol %. Therefore, the DPS molecules are interacting down to much lower graft site densities at low surface pressures than predicted by the de Gennes theory. Compared to the bilayers discussed below, the lipid density is low in monolayers at low surface pressure, which allows the PEG chains to spread at the air–water interface. Little difference between the isotherms of different DPS concentrations was observed at surface pressures above 20 mN/m. The lack of interactions at these higher surface pressures indicates that the repulsive pressure between adjacent grafted polymers is small compared to hard-core repulsion between the condensed aliphatic chains of the lipids in the monolayer. Repeated compression and expansion cycles reproduced the same isotherms, demonstrating reversibility and equilibrium of these monolayers (data not shown).

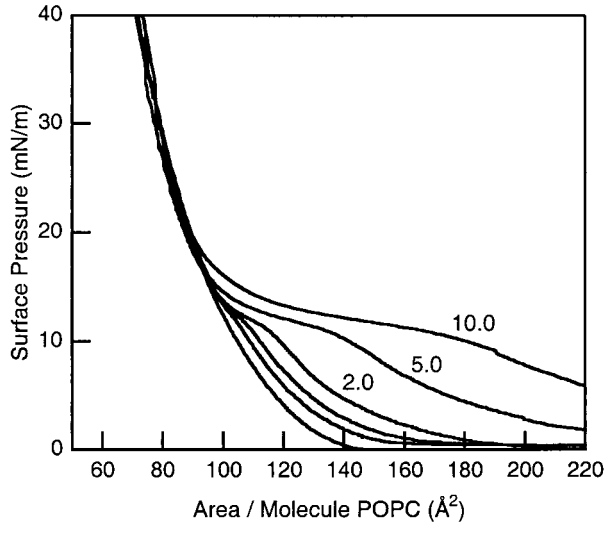

FIGURE 3 Pressure-area isotherms at 21°C of increasing mole fractions of DPS in monolayers of POPC on a Langmuir trough. Isotherms were recorded (*from left to right*) with 0, 0.5, 1.0, 2.0, 5.0, and 10.0 mol% DPS.

Polymer-supported planar lipid bilayers

To construct polymer-supported planar lipid bilayers, lipid monolayers composed of POPC and DPS were first deposited onto quartz by vertical immersion of quartz microscope slides through monolayers that were compressed to 32 mN/m on a Langmuir trough. The mole fractions of DPS were varied between 1% and 10%. Lipid transfer ratios (area removed from the air-water interface/surface area of the substrate) were routinely determined and found to be close to 100%, at all DPS concentrations. Polymer-supported planar bilayers were then completed by fusing unilamellar POPC vesicles to the supported monolayer (Kalb et al., 1992). Fig. 4 shows fluorescence micrographs of polymer-supported lipid bilayers taken at different times during the formation of bilayers with different concentrations of DPS. In these experiments, the inner DPS-containing monolayer was labeled with 2 mol% NBD-eggPE. Several interesting structural details that are unique to these polymer-supported bilayers were observed in the course of these experiments. At early times, when the bilayers were still incomplete, holes as well as two types of stripe defects were frequently observed. These defects "healed" within about 30 min as the lipid spread and the fluorescence became uniform across the entire field of view. The vertical striped patterns are due to the rheology and wetting behavior of the polymer because they were never observed in supported bilayers without the polymer and because they were always oriented parallel to the direction of coating of the monolayer on the Langmuir trough. As the concentration of DPS increased to 5 mol%, the vertical stripes became narrower and less prominent, until they were no longer laterally resolved by conventional epifluorescence microscopy. At very high concentrations of DPS, e.g., 10 mol% DPS as shown in Fig. 5 *A*, complex patterns appeared that persisted for very long times (days). These patterns, which were only observed well above the mushroom-to-brush transition of the polymer,

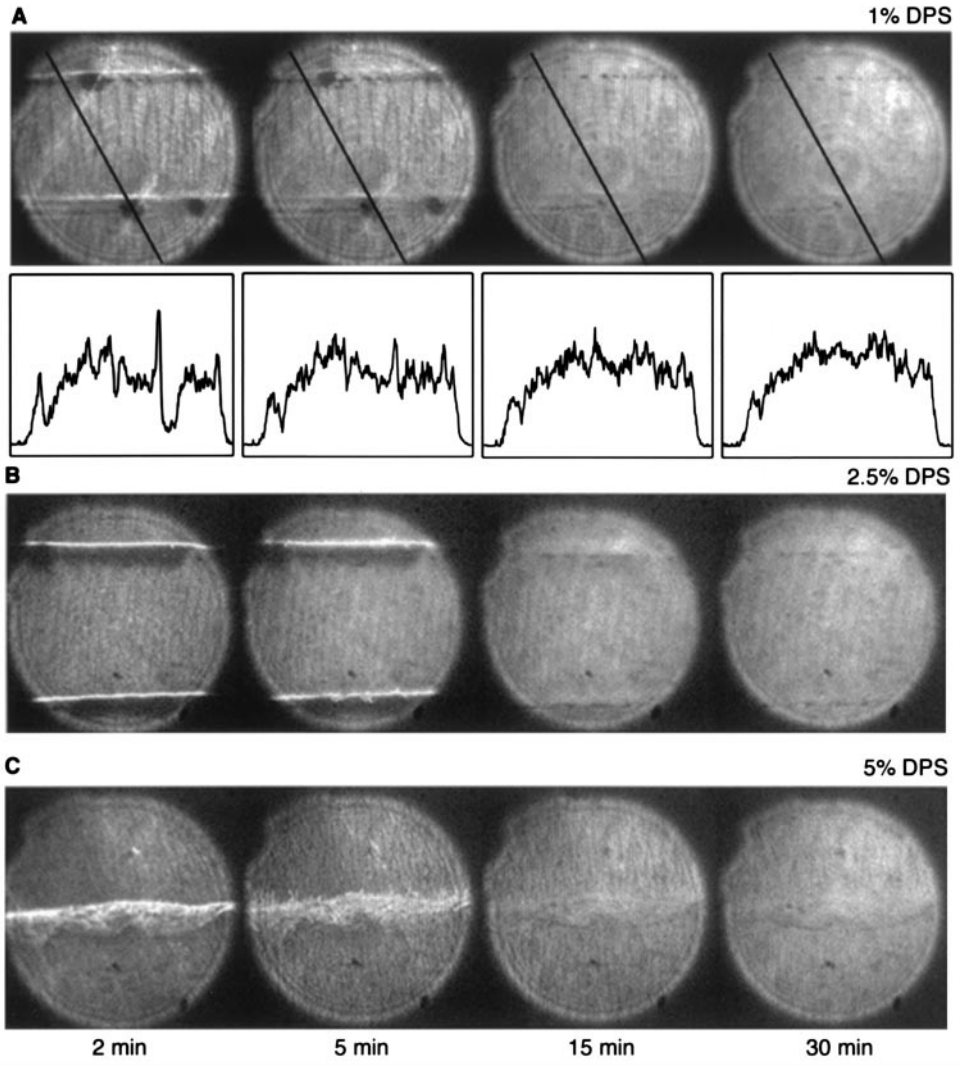

FIGURE 4 Epifluorescence micrographs of polymer-supported lipid bilayers during bilayer formation. The inner monolayer facing the solid substrate was labeled with 2 mol% NBD-eggPE. The concentrations of DPS in the inner monolayer are 1.0 mol% (*A*), 2.5 mol% (*B*), and 5.0 mol% (*C*). Different types of defects are seen to "heal" in the polymer-supported bilayers (see text for more detail). Fluorescence intensity profiles along the marked lines are shown in *A*. Illumination of the field is not uniform because of the Gaussian beam profile and interference patterns caused by out-of-focus objects in the path of the coherent laser light. The diameters of the circular observed areas are 150 μm.

reveal domain structures in bilayers on densely packed PEG. Our interpretation that these textures represent lipid domains with different partitioning capacities of NBD-eggPE is supported by photobleaching experiments as presented in Fig. 5 *B*. In these experiments, a stripe pattern was imaged onto the bilayer, and unprotected fluorophores were photolyzed by a brief pulse of laser light. The stripe patterns persisted for up to 1 h after removal of the bleaching mask and revealed better contrast between the darker and brighter lipid domains. Obviously, NBD-eggPE moved freely by lateral diffusion through the connected brighter domains but did not partition into the darker photobleached domains. When the outer monolayers were labeled with 2 mol% NBD-eggPE, uniform and almost defect-free fluorescence was observed at DPS concentrations up to 10 mol % (Fig. 5 *C*). The fluorescence in the photobleached areas recovered completely at 3 mol% and almost completely at 10 mol% 1 min after photobleaching.

To demonstrate lateral continuity and to probe the fluid-dynamic structure of the polymer-supported lipid bilayers, we measured lateral diffusion coefficients and mobile fractions of the lipids by FRAP. Fig. 6 shows these two parameters plotted as a function of the DPS concentration. The inner DPS-containing monolayer was labeled with 2 mol% NBD-eggPE in these experiments. In the low and high DPS concentration regimes, the lateral diffusion coefficients were high (1–1.5 $\times$ 10^{-8} cm^2/s), i.e., comparable to those previously measured in bilayers that were directly supported on silicate substrates (Tamm, 1988; Kalb et al., 1992). The mobile fractions were also high (70–80%) up to ~4 mol% DPS, but decreased to ~50% in a relatively sharp transition above 4 mol% DPS. Within and close to this transition region the lipid lateral diffusion coefficients were slightly decreased to ~0.7 $\times$ 10^{-8} cm^2/s. Because all FRAP recovery curves were fit to single exponentials (corresponding to a single diffusing species), it is possible that the measured

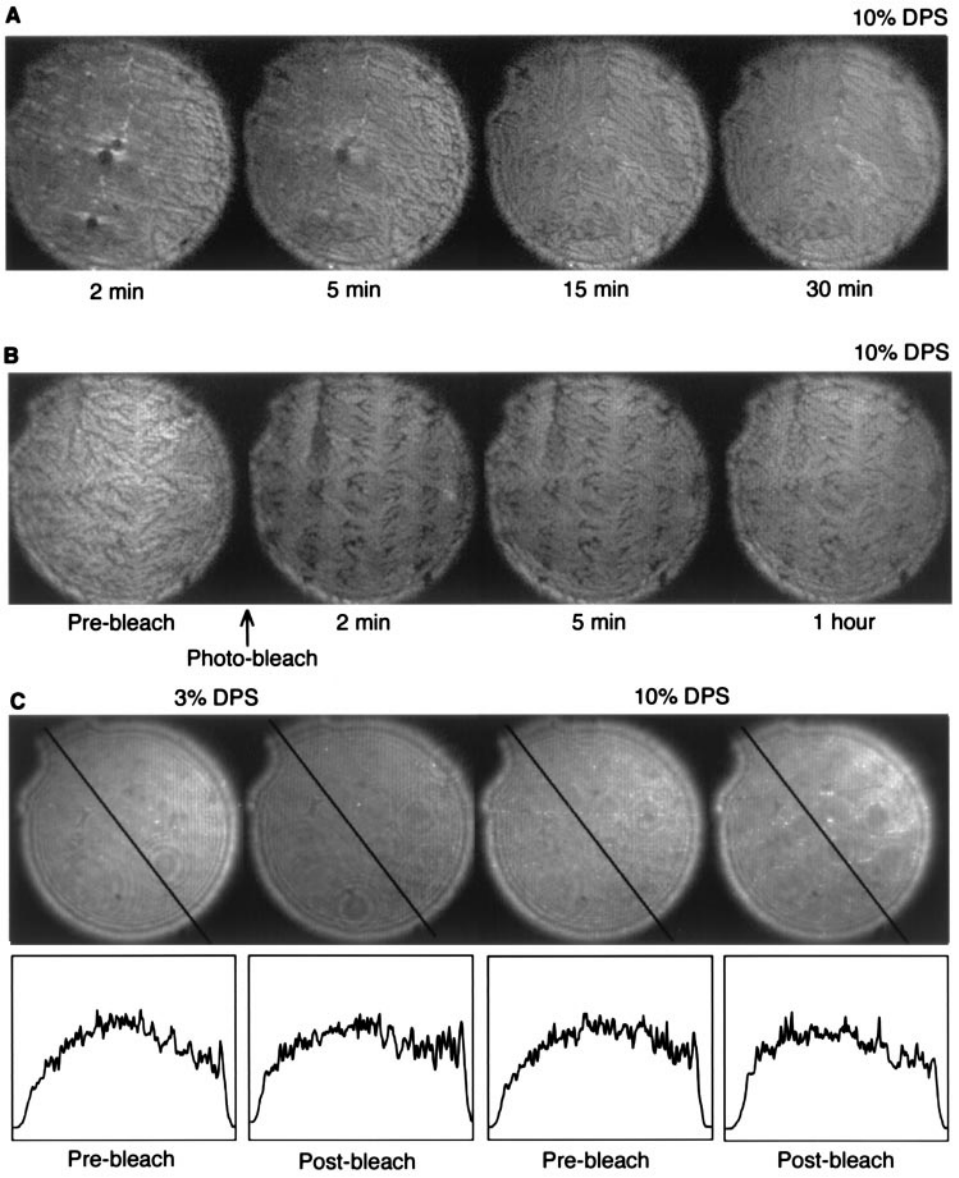

FIGURE 5 Epifluorescence micrographs of polymer-supported lipid bilayers containing 10 or 3 mol% DPS. (*A*) The inner monolayer facing the solid substrate was labeled with 2 mol% NBD-eggPE. A distinct pattern of fluorescence distribution persists at this concentration of DPS. (*B*) A sequence of images of a different area of the same bilayer as in *A*, before and 2, 5, and 60 min after a stripe pattern was photobleached into the membrane. This experiment enhances the contrast between membrane domains of fast and slow diffusing NBD-eggPE in lipid bilayers that are supported by a dense polymer brush. (*C*) The outer monolayer facing the large aqueous compartment was labeled with 2 mol% NBD-eggPE. The fluorescence distributions are uniform in these samples (see legend to Fig. 4 for effects caused by laser illumination). The fluorescence has equilibrated completely (3 mol%) or almost completely (10 mol%) 1 min after a stripe pattern was photobleached into these membranes (*second and forth micrographs in this series*). The diameters of the circular observed areas are 150 μm.

lower diffusion coefficients in the transition region actually represent two unresolved diffusion processes that might be expected in a two-component system. The slower component becomes completely immobilized on the time scale of these particular FRAP experiments only above 6 mol% DPS. At this same threshold, we begin to see the domains that were presented in Fig. 5. The loss of mobile fraction correlates quite well with the mushroom-to-brush transition of the supporting polymer as predicted by the de Gennes scaling theory (Fig. 2). However, the lipid diffusion coefficients report on a broader transition than predicted by the idealized two-state transition, perhaps because they are more sensitive to subtle changes in the underlying polymer. Lateral diffusion of lipids in the outer monolayer was only measured at 3 and 10 mol% DPS, i.e., the conditions of the images shown in Fig. 5 *C*. The lateral diffusion coefficients were close to 1×10^{-8} cm^2/s at both DPS concentrations, but the mobile fraction decreased from 68.0 ± 1.1 to 52.8 ± 4.7 when the DPS concentration was increased from 3 to 10 mol%. Table 1 compares the diffusion properties of the lipids in the outer monolayer with those of the inner monolayer on different supports. The lateral diffusion coefficients and mobile fractions of the outer monolayers closely matched those of the inner monolayer for each polymer condition that was examined in this regard. The results of Figs. 4, 5, and 6 and Table 1 show that a polymer concentration just below the mushroom-to-brush transition holds the most promise for the reconstitution of integral membrane proteins into polymer-supported lipid bilayers. Therefore, we chose 3 mol% DPS for further experiments to examine the effect of covalent tethering of the polymer to the substrate and the reconstitution of membrane proteins

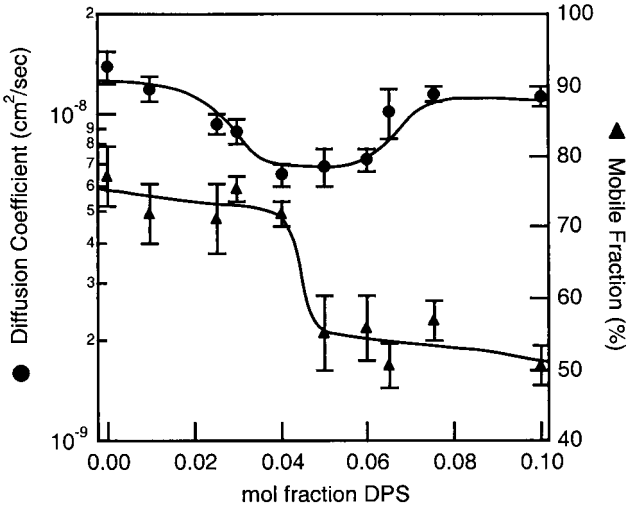

FIGURE 6 Lateral diffusion of the lipid probe NBD-eggPE in DPS-supported POPC bilayers as a function of DPS concentration. The lateral diffusion coefficients and mobile fractions undergo transitions near the predicted mushroom-to-brush transition. The inner monolayer facing the solid substrate was labeled with 2 mol% NBD-eggPE. Each data point represents the average of 15–20 measurements from three different bilayers.

into cured (tethered) and uncured (partially tethered) polymer-supported lipid bilayers.

Tethered polymer-supported planar lipid bilayers

Covalent tethering of the DPS molecule by curing the silane moiety to the free silanols of the quartz slide was examined via XPS. A pure DPS monolayer was transferred onto quartz as described above, cured at 70°C for 40 min, and analyzed by XPS (Fig. 7). Spectra of a clean quartz surface, a monolayer of PEG2000-DMPE (PEG lipid without the silane linker), and an uncured DPS monolayer are also shown for comparison. In these experiments any noncovalently linked molecules were removed by thoroughly rinsing the surface with methanol before XPS spectra were recorded. The spectra show the energies of electrons that are released from several shells (as assigned) of the different elements that are present on the surface of each sample. The pure quartz and PEG2000-DMPE samples show strong oxygen peaks, whereas carbon peaks dominate the spectrum of the DPS sample. Because photoelectron spectra are dominated by the elements that are present at the very surface of the sample, we conclude that in contrast to cured DPS, PEG2000-DMPE did not bind to quartz. The uncured DPS sample exhibits an intermediate carbon/oxygen ratio, indicating that even without curing DPS partially reacts with the surface. The C_{1s} peak that arises from the carbon valence electrons can be further energy-analyzed for different covalent bonds that carbon forms in the sample (Fig. 7, *inset*). This peak displays a major component with a binding energy of 286.0 eV, i.e., very similar to the carbon value previously reported for PEG (Thomas and O'Malley, 1979). The other major component at 287.8 eV is characteristic for carbon ester groups in DMPE. A ratio of 2.3:1 was determined from the areas under the PEG peaks of C_{1s} and O_{1s} (286.5 and 533.3 eV), respectively, after calibration with appropriate sensitivity factors. This ratio is very close to the 2:1 ratio previously reported for the surface of solid PEG (Thomas and O'Malley, 1979).

Tethered polymer-supported lipid bilayers composed of POPC and 3 mol% DPS in the inner leaflet and 2 mol% NBD-eggPE in the outer leaflet were prepared as described in Materials and Methods. They appeared uniform by epifluorescence microscopy, as shown in Fig. 5 *C* for corresponding uncured polymer-supported bilayers. Lateral diffusion experiments resulted in a lateral diffusion coefficient of $(0.89 \pm 0.08) \times 10^{-8}$ cm^2/s and a mobile fraction of $66.5 \pm 1.4\%$, i.e., not much different from the values measured in the corresponding uncured DPS-supported bilayers (Table 1).

Reconstitution and lateral diffusion of cytochrome b_5

Cytochrome b_5 is a two-domain protein with a small globular domain ($M_r \approx 11{,}000$) and a hydrophobic peptide ($M_r \approx 4200$) that penetrates deep into the lipid bilayer. We chose this protein as our first test integral membrane protein for its relatively simple architecture and ready availability. Fluorescein-labeled cytochrome b_5 was reconstituted into supported bilayers at a lipid/protein ratio of 40:1 by fusion of proteoliposomes ($L/P = 20{:}1$) to the supported monolayers (see Materials and Methods). Uniformly fluorescent bilayers were obtained on quartz, on DPS cushions, and on tethered DPS cushions (Fig. 8 *A*, *first image from left*). We measured the lateral mobilities of cytochrome b_5 by FRAP in all three systems and inspected epifluorescence micrographs with photobleached stripe patterns for extended periods of time to detect more slowly diffusing components. An example of a FRAP curve of cytochrome b_5 in a tethered polymer-supported bilayer is shown in Fig. 8 *B*. Twenty-seven percent of the reconstituted cytochrome b_5 diffused with a lateral diffusion coefficient of 1.4×10^{-8} cm^2/s. Fifty to sixty percent of the fluorescence recovered over a time scale of ~10 min, as is evident from the slow disappearance of the bleached stripes shown in Fig. 8 *A*. The lateral diffusion coefficient of this slower component is estimated from these micrographs to be $\sim 2 \times 10^{-10}$ cm^2/s. The remaining 10–20% of cytochrome b_5 was immobile, even on this time scale. This minor fraction could be due to aggregated protein or some protein that is immobilized in small invisible defects in the bilayer. In contrast to cytochrome b_5 in the polymer-supported bilayers, cytochrome b_5 in bilayers that were directly supported on quartz showed a smaller mobile fraction (20%) of the faster component

TABLE 1 Lateral mobility of NBD-eggPE in solid, polymer-supported, and tethered polymer-supported lipid bilayers*

Type of support	NBD-PE labeled	$n^{\dagger}$	Diffusion coefficient ($\times 10^{-8}$ cm^2/s)	Mobile fraction (%)
Glass	Inner leaflet	13	1.39 ± 0.15	77.4 ± 4.1
	Outer leaflet	5	1.32 ± 0.07	84.5 ± 0.1
3% DPS cushion	Inner leaflet	18	0.88 ± 0.08	75.4 ± 1.8
	Outer leaflet	5	1.04 ± 0.04	68.0 ± 1.1
10% DPS cushion	Inner leaflet	15	1.13 ± 0.08	50.5 ± 2.9
	Outer leaflet	5	0.89 ± 0.05	52.8 ± 4.7
3% DPS tether	Inner leaflet	—	ND‡	ND
	Outer leaflet	5	0.89 ± 0.08	66.5 ± 1.4
3% DPS tether	Inner leaflet	—	ND	ND
(1:83 mol/mol Cyt b_5)	Outer leaflet	5	0.50 ± 0.08	70.1 ± 4.4

*Bilayers were composed of POPC with 2 mol% NBD-eggPE in one leaflet and the appropriate mole fraction of DPS in the inner leaflet as indicated.
†No. of experiments.
‡Not determined.

(Fig. 8 *B, dashed line*), and the remaining 80% of cytochrome b_5 was laterally immobile on the 10–30-min time scale. Lateral diffusion coefficients and mobile fractions averaged from more experiments of cytochrome b_5 in the three different types of supported bilayers are listed in Table 2. Similar data were also obtained at protein concentrations that were two or five times smaller. The lateral diffusion coefficients and mobile fractions of 2 mol% NBD-eggPE that were included in the outer monolayer were unaffected or only slightly reduced by the presence of unlabeled cytochrome b_5 that was reconstituted at a lipid/protein ratio of 83:1 (Table 1).

Binding and lateral diffusion of annexin V

As an example of a multihelical protein that binds to and likely penetrates lipid bilayers to some degree in a Ca^{2+}-dependent fashion, we investigated the bilayer morphology and diffusion behavior of annexin V in negatively charged

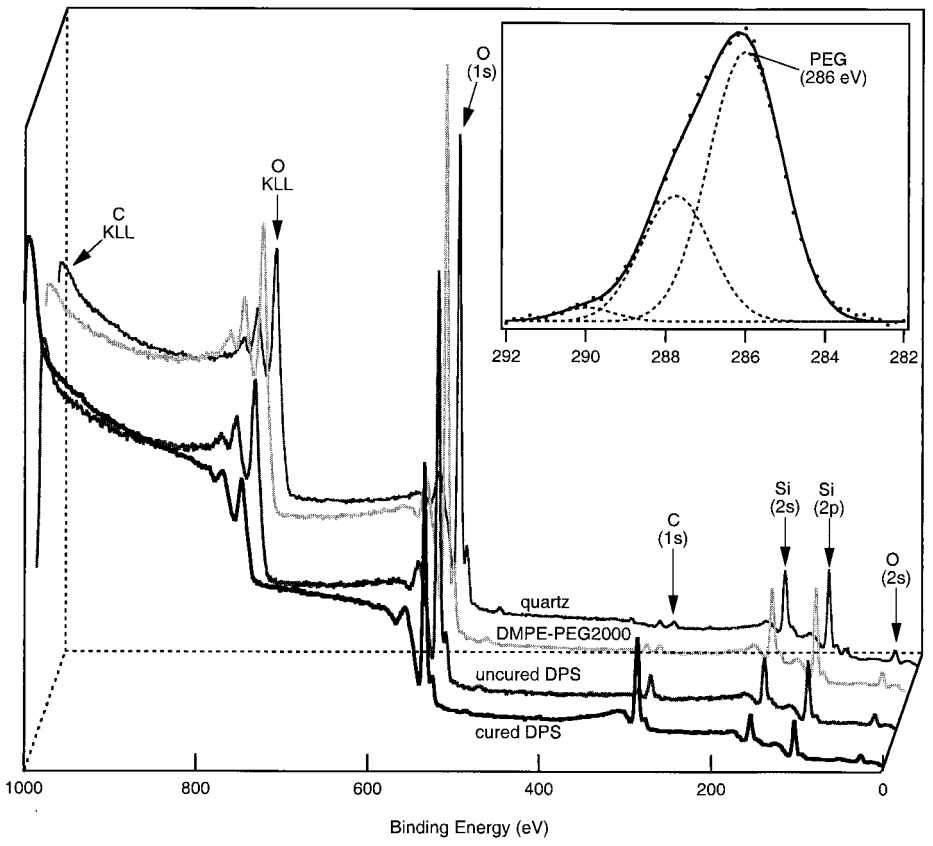

FIGURE 7 X-ray photoelectron spectra demonstrating the covalent tethering of the DPS molecule to the quartz surface. The spectra from front to back were obtained with a cured sample of DPS, an uncured sample of DPS, a sample of PEG2000-DMPE, and a pure quartz surface, respectively. The samples with the monolayers were washed with methanol to remove noncovalently bound polymer lipids. Peaks from the KLL and valence electron shells of the different elements are assigned as marked. The inset shows an analysis of the C_{1s} peak with a fit to three Gaussian components ($\chi^2 = 1.3 \times 10^{-4}$). The main component at 286.0 eV is assigned to PEG, and the second largest component at 287.8 eV is assigned to the carbon ester groups of the lipid.

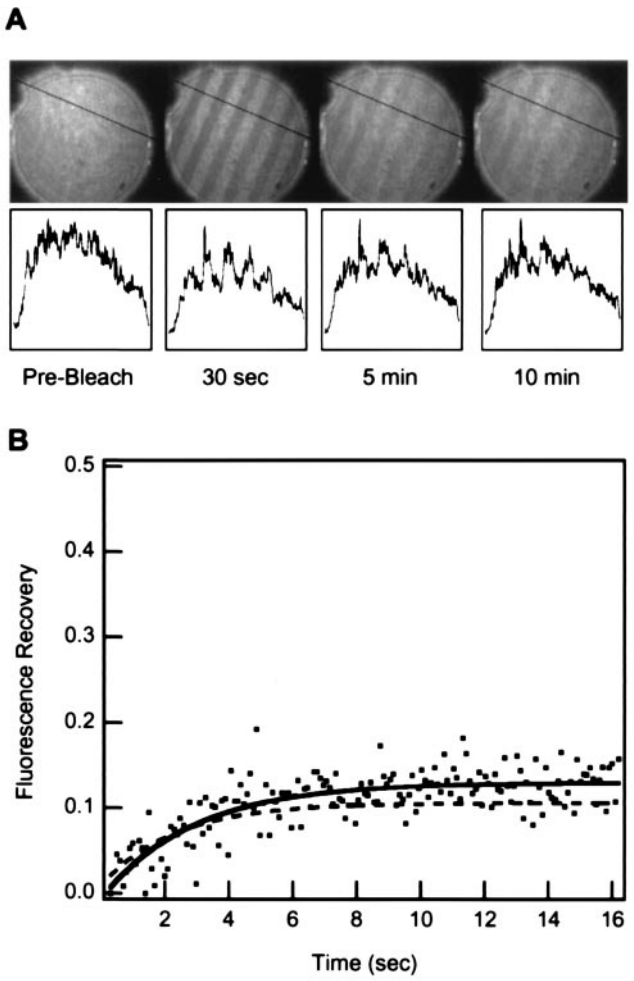

FIGURE 8 Lateral diffusion of cytochrome b_5 in a tethered DPS-supported lipid bilayer. (*A*) Epifluorescence micrographs (diameter 150 μm) showing the distribution of fluorescein-labeled cytochrome b_5 reconstituted in a tethered DPS-supported POPC bilayer before and 30 s, 5 min, and 10 min after a periodic stripe pattern was bleached into the membrane. This experiment reveals a slowly ($\sim 2 \times 10^{-10}$ cm^2/s) diffusing component of cytochrome b_5. The DPS concentration in the inner, substrate-exposed monolayer was 3 mol%, and the lipid/protein ratio was 40:1. (*B*) FRAP experiment of the same bilayer as in *A*, showing a fast (1.4×10^{-8} cm^2/s) diffusing component of cytochrome b_5. The solid line is a single exponential fit to the experimental data. The dashed line is shown for comparison and shows a single exponential fit of a FRAP experiment performed on cytochrome b_5 that was reconstituted into a quartz-supported lipid bilayer without a polymer cushion. The more slowly diffusing component is not observed (immobile) under these conditions.

bilayers on different supports. Fluorescein-labeled annexin V was bound from solution to preformed asymmetrical POPC/POPC:POPG (9:1) bilayers on pure quartz, DPS/quartz, and tethered DPS/quartz in the presence of 1 mM Ca^{2+}. A saturating concentration of 56 nM annexin V was used in all three cases. The fluorescence distribution was homogeneous for annexin V bound to all three types of supported bilayers (Fig. 9 *A*). As observed with cytochrome b_5, FRAP experiments showed two components of membrane-bound annexin V with different lateral mobilities. A faster component was observed (Fig. 9 *B* and Table 2), which corresponded to 21%, 45%, and 33% of the bound annexin V on the quartz-supported, the DPS-supported, and the tethered DPS-supported bilayers, respectively. The lateral diffusion coefficients of these components ranged from 1.6×10^{-9} to 3.0×10^{-9} cm^2/s, i.e., they were about three to six times slower than the faster components of cytochrome b_5 (Table 2). As with cytochrome b_5, a more slowly diffusing component was observed with annexin V (Fig. 9 *A*). The fluorescence recovered completely after 5–10 min, resulting in a diffusion coefficient of $\sim 4 \times 10^{-10}$ cm^2/s, i.e., about twice as fast as the slow component of cytochrome b_5 (Table 2). No immobile components were observed for annexin V on the tethered polymer-supported bilayers, while 70–80% of annexin V was immobile on quartz-supported bilayers.

DISCUSSION

We have produced a new tethered polymer-supported lipid bilayer system that increases the mobile fraction of some membrane proteins when integrated or bound to supported lipid bilayers. A PEG cushion with the ends of the linear polymer covalently linked to the hydrophilic solid support and the membrane, respectively, proved successful. Uniformly fluorescent bilayers exhibiting nearly unrestricted lipid diffusion in both leaflets of the bilayer were obtained on cushions of moderate polymer density. Two test proteins, cytochrome b_5 and annexin V, retained almost full lateral mobility when bound to or inserted into the polymer-supported bilayers. Both proteins exhibited two-component lateral diffusion on the soft supports with an unrestricted and a partially restricted component. When directly supported on quartz or glass, the slower diffusion components of both proteins were completely immobilized, demonstrating the ability of the PEG cushion to detach the proteins from the solid support.

Cytochrome b_5 and annexin V are thought to insert into lipid bilayers by different modes of interaction. Cytochrome b_5 has a single hydrophobic helical peptide that penetrates deep into the lipid bilayer (Holloway and Buchheit, 1990; Ladokhin and Holloway, 1991, 1995). Whether it actually spans the entire thickness of the lipid bilayer is still a matter of debate, although the most recent data support a transbilayer orientation (Vergères et al., 1995). In any case, we observe $\sim$25% of cytochrome b_5 diffusing with a lateral diffusion coefficient of $\sim 1.3 \times 10^{-8}$ cm^2/s on the tethered polymer cushions (Table 2). This is as fast as the lipids themselves in the same system (Fig. 6 and Table 1) and is typical of unrestricted protein diffusion in a lipid bilayer. Fifty to sixty percent of cytochrome b_5 diffuses with a lateral diffusion coefficient of $\sim 2 \times 10^{-10}$ cm^2/s on the polymer. The most straightforward explanation for the 60–70-fold lower lateral diffusion coefficient of this population

TABLE 2 Lateral mobility of cytochrome b_5 and annexin V in quartz-supported, polymer-supported, and tethered polymer-supported lipid bilayers

			Faster component (FRAP)		Slower component (image analysis)	
Type of support	Protein	n*	Diffusion coefficient ($\times 10^{-8}$ cm^2/s)	Mobile fraction (%)	Diffusion coefficient	Mobile fraction
Quartz	Cytochrome b_5†	11	1.13 ± 0.47	22.7 ± 5.7	—§	0
	Annexin V‡	10	0.18 ± 0.10	21.0 ± 8.0	—§	0
DPS cushion	Cytochrome b_5†	9	0.44 ± 0.06	28.2 ± 3.3	ND¶	ND
	Annexin V‡	15	0.16 ± 0.08	45.2 ± 3.6	ND	ND
DPS tether	Cytochrome b_5†	10	1.32 ± 0.65	26.4 ± 2.4	$\sim 2 \times 10^{-10}$ cm^2/s	50–60%
	Annexin V‡	21	0.30 ± 0.10	33.3 ± 6.5	$\sim 4 \times 10^{-10}$ cm^2/s	60–70%

*No. of experiments from at least three different samples in each situation.
†In POPC bilayers with lipid/protein ratios of 20:1 in outer leaflet or 40:1 overall.
‡The outer monolayers were composed of POPC:POPG (9:1), and 56 nM fluorescein-labeled annexin V was allowed to bind in the presence of 1 mM Ca^{2+} before unbound annexin V was removed by washing the cell with a 1 mM Ca^{2+}-containing buffer. Ca^{2+} did not affect diffusion of the lipids (data not shown, but see Gilmanshin et al., 1994).
§Components equal to or faster than 5×10^{-12} cm^2/s would have been easily detected in these experiments.
¶Not determined.

of restricted lateral mobility is that the molecules of this pool interact weakly with the underlying polymer network. Bulk diffusion measurements as used in this study cannot provide detail on the interactions of individual molecules with the polymer. It is possible that molecules in this more slowly diffusing population transiently attach and detach from the polymer. The net result of a FRAP experiment in such a scenario could well be a diffusion coefficient on the order of 10^{-10} cm^2/s, as observed. Single-molecule experiments would be needed to detect inhomogeneous motions in supported bilayers (Schütz et al., 1997). Interestingly, many integral membrane proteins in cell membranes diffuse with a similar slow rate, and their lateral mobilities are thought to be restricted by interactions with the underlying polymerized network of the cytoskeleton (Edidin et al., 1994; Saxton and Jacobson, 1997). Evans and Sackmann (1988) extended the Saffmann-Delbrück equations for the lateral diffusion of membrane proteins to the situation where friction between the protein and the bathing medium (polymer in our case) is not negligible compared to the viscous drag within the lipid bilayer. Under such conditions they find

$$D_L^{-1} = \frac{4\pi\eta_m}{kT}\left[\frac{\epsilon^2}{4} - \epsilon\frac{K_1(\epsilon)}{K_0(\epsilon)}\right] \qquad (6)$$

$$\epsilon = R\sqrt{\eta_w/(\eta_m d_w)}$$

where D_L is the lateral diffusion coefficient, η_m and η_w are the microviscosities of the membrane and bathing solutions, respectively, R is the radius of the diffusing particle (approximated as a cylinder), d_w is the thickness of the lubricating aqueous film, and $K_{0,1}$ are Bessel functions of the second kind. The first term in brackets in Eq. 6 describes the coupling between the diffusing particle and the bathing solution, and the second term corresponds to the classical Saffman-Delbrück logarithmic law. When the coupling becomes the dominant factor ($\epsilon \gg 1$) determining diffusion, we can estimate the viscous drag that is exerted by the polymeric film on the protein from the approximation

$$D_L \approx \frac{kTd_w}{\pi\eta_w R^2} \qquad (7)$$

Using a radius of 6 Å for the helix of cytochrome b_5, we calculate a frictional coefficient η_w/d_w of 1.80×10^7 dyn s/cm^3 for the interaction of the protein with the polymer film. Assuming further that the polymer film is 50 Å thick ($\approx$ or $>$ Flory radius), we obtain a microviscosity of 9 Poise in the polymer film. This is about nine times larger than the microviscosity that the protein experiences in the lipid bilayer itself (Vaz et al., 1984). The "microviscosity" determined using a protein as a probe in a relatively dense polymer is likely to scale with the size of the probe (protein), the thickness of the film, and the density of the polymer. It should therefore not be considered a universal "material constant" for this system.

Annexin V is a disk-shaped molecule consisting of four domains of five helices each that are arranged around a pseudofourfold symmetry axis (Huber et al., 1990). The protein binds to negatively charged bilayers in a Ca^{2+}-dependent fashion with its disk oriented parallel to the membrane surface. It also has the ability to crystallize in two-dimensional lattices on membrane surfaces (Voges et al., 1994; Reviakine et al., 1998). Among the proposed functions of annexin V and other members of the annexin family are their involvement in membrane fusion in Ca^{2+}-triggered exocytosis, vesicular trafficking, and ion channel formation (Seaton, 1996). These functions suggest that the interaction of annexins with lipid bilayers may be more intimate than purely electrostatic. For example, annexin V induces Ca^{2+}-selective channels in lipid bilayers (Berendes et al., 1993) and significantly reduces the lateral diffusion of

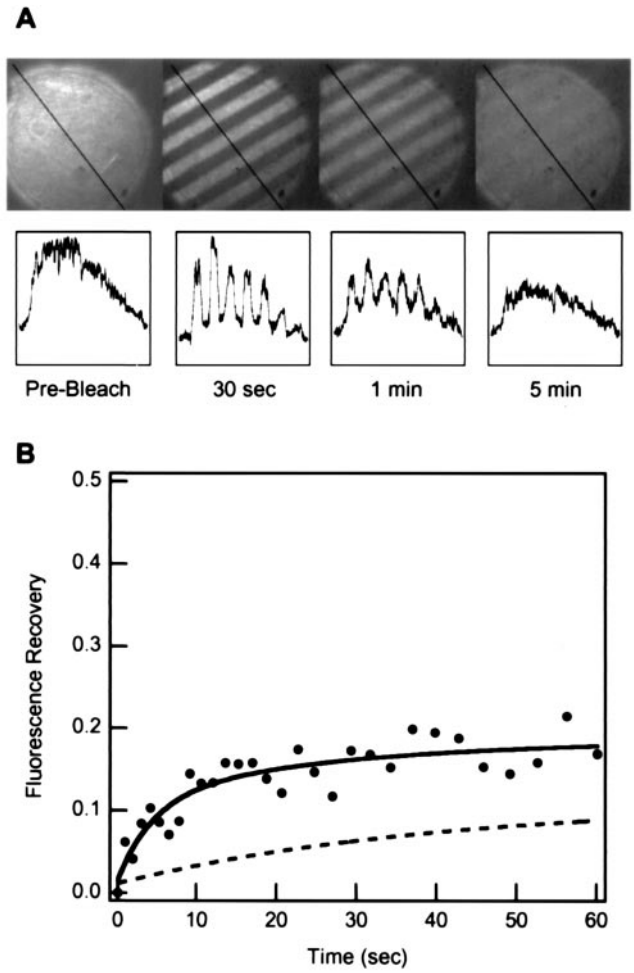

FIGURE 9 Lateral diffusion of annexin V in a tethered DPS-supported lipid bilayer. (*A*) Epifluorescence micrographs (diameter 150 μm) showing the distribution of fluorescein-labeled annexin V bound from a 56 nM solution in the presence of 1 mM Ca^{2+} to an asymmetrical tethered DPS-supported POPC/POPC:POPG (9:1) bilayer before and 30 s, 1 min, and 5 min after a periodic stripe pattern was bleached into the membrane. This experiment reveals a slowly diffusing ($\sim 4 \times 10^{-10}$ cm^2/s) component of annexin V. The DPS concentration in the inner, substrate-exposed monolayer was 3 mol%. (*B*) FRAP experiment of the same bilayer as in *A*, showing a relatively fast (4×10^{-9} cm^2/s) diffusing component of annexin V. The solid line is a single exponential fit to the experimental data. The dashed line is shown for comparison and shows a single exponential fit of a FRAP experiment performed on annexin V that was bound to a quartz-supported lipid bilayer without a polymer cushion. The more slowly diffusing component is not observed (immobile) under these conditions.

lipids in artificial lipid bilayers (Gilmanshin et al., 1994; Cézanne et al., 1999). Recent evidence from site-directed spin-labeling, photoaffinity labeling, and Triton X-114 partitioning shows that under mildly acidic conditions annexins V and XII penetrate lipid bilayers completely in a binding reaction that involves a fully reversible conformational change (Langen et al., 1998; Isas et al., 2000). As for cytochrome b_5, we found two-component diffusion of annexin V in tethered polymer-supported bilayers. However, the faster component ($\sim$33%) is slower ($\sim 3 \times 10^{-9}$ cm^2/s, Table 2) than that of cytochrome b_5. This diffusion coefficient is similar to that of the lipids themselves in a 10 mol% POPG bilayer with bound annexin IV (Gilmanshin et al., 1994) and reflects a general change in the dynamic properties of the lipid bilayer in the presence of annexins. The slower component (60–70%) is similar to that of cytochrome b_5 ($\sim 4 \times 10^{-10}$ cm^2/s) and is induced by the polymer. This component is immobile in the absence of the polymer. The restricted mobility of annexin V may simply be caused by its tendency to self-associate laterally on membrane surfaces. Crystallization on hard-supported bilayers may be more complete than that on soft-supported bilayers. Alternatively, annexin may partially penetrate the bilayer in a reversible Ca^{2+}-dependent fashion. Using the same approach as above for cytochrome b_5, we calculate a frictional coefficient of 5.6×10^5 dyn s/cm^3 and a microviscosity of 0.28 Poise. These values are much lower than the corresponding values of cytochrome b_5, which is consistent with the notion that annexin V interacts weakly with the polymer layer but does not significantly penetrate it.

The structure of PEG grafted onto lipid monolayers has been studied previously at the air-water interface of a Langmuir trough or in supported monolayers by x-ray and neutron reflectometry, as well as by thermodynamic and microfluorescence techniques (Baekmark et al., 1995; Kuhl et al. 1994, 1998; Majewski et al., 1997, 1998a; Rex et al., 1998). The geometry and goals of these previous studies were fundamentally different from those of the present work. The major focus of these previous studies was on the behavior of the grafted PEG chains that were facing the aqueous solution away from the substrate. In contrast, in the present work we have studied polymers that are sandwiched between the solid support and a fluid membrane. Several important results emerged from the previous studies on the grafted polymers that may also be relevant for sandwiched tethered polymers. Transitions between the "mushroom" and "brush" states of the polymer were clearly revealed in the monolayer systems. For example, the extension lengths of the polymer above the surface increased upon going from 4.5% (mushroom) to 9% (brush) PEG2000-DSPE from 40 to 70 Å when measured with the surface force apparatus (Kuhl et al., 1994) or from 45 to 60 Å when measured by neutron reflectometry (Kuhl et al., 1998). PEG2000-DSPE has 45 monomer units and consequently a smaller Flory radius (35 Å) than our DPS molecule. Therefore, even below the mushroom-to-brush transition these polymers appear to be slightly more extended than anticipated from the simplistic de Gennes–Flory prediction. This result agrees with the finding that the PEG chains begin to interact with one another already at relatively low surface densities, which can be seen in the Langmuir pressure-area isotherms that were previously published for PEG2000-DSPE by several authors (Baekmark et al., 1995; Majewski et al., 1997, 1998a) and are reproduced here for DSP (Fig. 3). In this

context, it is interesting to note that we observed a transition of lateral lipid diffusion around 4–5 mol% DPS (Fig. 6). Although detected indirectly by the fluid dynamic behavior of the grafted lipid bilayer, this may be the first experimental evidence for a mushroom-to-brush transition in a thin, sandwiched polymer film.

An interesting and, for practical applications, useful property of the DSP-supported bilayers is that they appear to "heal" small defects more readily than lipid bilayers that are directly supported on quartz or glass (Fig. 4). Circular defects like those seen in Fig. 4 *A* (*first micrographs from the left*) are sometimes observed in silicate-supported bilayers (see, e.g., Tamm and McConnell, 1985). However, they seem to be more permanent on the hard hydrophilic supports, where they usually do not disappear once they are formed. The smaller vertical line defects of Fig. 4, *A* and *B*, are not observed in silicate-supported bilayers, but they appear to heal quite well in the PEG-supported bilayers under neutral pH conditions. A low pH-induced healing of supported bilayers over mechanically induced scratches on glass surfaces has been described in quite some detail (Cremer and Boxer, 1999; Cremer et al., 1999). We do not fully understand the mechanism(s) of the healing process(es) in our polymer-supported bilayer system. It is possible that the polymers mask imperfections on the solid substrate and thereby provide for a smoother and more dynamic surface for vesicle spreading. The line defects and their slow disappearance may also be caused by draining and partial drying of the polymer during the Langmuir-Blodgett deposition of the inner monolayer and the subsequent (slow?) rehydration of the polymer during vesicle spreading. Whatever the mechanism, the healing capacity of all observed defects seems greatest just below the mushroom-to-brush transition, which is the main reason why we chose 3 mol% DPS as our optimal polymer concentration. When supported on PEG in the brush region (10 mol% DPS), the bilayer segregates laterally into microscopic but connected lipid domains (Fig. 5, *A* and *B*). It is likely that these domains reflect underlying lateral heterogeneities of the polymer brush. The domains are striped, with the stripes orientated perpendicular to the Langmuir-Blodgett coating direction. Although the mobile fractions (and diffusion coefficients) are almost the same when the inner or outer monolayers on 10 mol% DPS are labeled (Table 1), the fluorescence distribution in the outer monolayer is more uniform than in the inner monolayer (Fig. 5, *A* and *C*). This could indicate a mismatch between lipid domains of the inner and outer monolayers. Alternatively, vesicle spreading may fill preexisting holes or defects in the inner monolayer. Even if the structures seen in Fig. 5, *A* and *B*, persist for more than an hour, they could still be kinetically trapped, rather than equilibrium structures. More work is needed to sort out these various possibilities. However, because the focus of the present study was to find the best and most uniform bilayer conditions for membrane protein reconstitution, we did not attempt to further characterize bilayers on polymer brushes.

In conclusion, we have shown that PEG-lipids that are covalently tethered to the surface of silicate substrates at appropriate concentrations form viable cushions for supported lipid bilayers with long-range order and long-term stability. Most importantly, these cushions support full lateral diffusion of two membrane proteins that are not free to diffuse when bound to or incorporated into glass- or quartz-supported bilayers. However, a significant fraction of these membrane proteins exhibit restricted lateral diffusion, presumably because of their viscous coupling to the polymer support. The restricted diffusion coefficients are on the order of 10^{-10} cm^2/s and resemble those measured for many integral membrane proteins in cells. The viscous coupling of proteins to the PEG polymer may thus resemble the viscous coupling of membrane proteins to the underlying cytoskeleton in cells. We do not know yet whether our design of polymer-supported bilayers can be generalized to the functional reconstitution of other membrane proteins and receptors with larger hydrophilic domains. Further refinements of methods may be required to achieve this general goal. The structure of the polymer-supported bilayers also needs to be investigated at higher resolution by appropriate techniques. This will be an effort well worth undertaking and complementary to the morphological and fluid dynamic characterization of the bilayers with and without proteins that we have presented in this work. We believe that our new approach to membrane protein reconstitution into polymer-supported bilayers constitutes a further step toward faithfully mimicking cell surfaces under controlled conditions on artificial supports.

We thank Dr. Peter Holloway for the kind gift of cytochrome b_5, Catherine Dukes for help with the XPS experiments, and members of the Tamm laboratory for numerous helpful discussions.

REFERENCES

Ames, B. N. 1966. Assays of inorganic phosphate, total phosphate and phosphatases. *Methods Enzymol.* 8:115–118.

Ariga, K., J. S. Shin, and T. Kunitake. 1995. Interaction of lipid monolayers with aqueous neutral polymers and consequent monolayer stabilization and improved Langmuir Blodgett transfer. *J. Colloid Interface Sci.* 170:440–448.

Arnold, K., O. Zschoernig, D. Barthel, and W. Herold. 1990. Exclusion of poly(ethylene glycol) from liposome surfaces. *Biochim. Biophys. Acta.* 1022:303–310.

Baekmark, T. R., G. Elender, D. D. Lasic, and E. Sackmann. 1995. Conformational transitions of mixed monolayers of phospholipids and poly(ethylene oxide) lipopolymers and interaction forces with solid surfaces. *Langmuir.* 11:3975–3987.

Berendes, R., D. Voges, P. Demange, R. Huber, and A. Burger. 1993. Structure-function analysis of the ion channel selectivity filter in human annexin V. *Science.* 262:427–430.

Beyer, D., G. Elender, W. Knoll, M. Kühner, S. Maus, H. Ringsdorf, and E. Sackmann. 1996. Influence of anchor lipids on the homogeneity and

mobility of lipid bilayers on thin polymer films. *Angew. Chem. Int. Ed. Engl.* 35:1682–1685.

Cézanne, L., A. Lopez, F. Loste, G. Parnaud, O. Saurel, P. Demange, and J.-F. Tocanne. 1999. Organization and dynamics of the proteolipid complexes formed by annexin V and lipids in planar supported lipid bilayers. *Biochemistry.* 38:2779–2786.

Cornell, B. A., V. L. B. Braach-Maksvytis, L. G. King, P. D. J. Osman, B. Raguse, L. Wieczorek, and R. J. Pace. 1997. A biosensor that uses ion-channel switches. *Nature.* 387:580–583.

Cremer, P. S., and S. G. Boxer. 1999. Formation and spreading of lipid bilayers on planar glass supports. *J. Phys. Chem. B.* 103:2554–2559.

Cremer, P. S., J. T. Groves, L. A. Kung, and S. G. Boxer. 1999. Writing and erasing barriers to lateral mobility into fluid phospholipid bilayers. *Langmuir.* 15:3893–3896.

de Gennes, P. G. 1987. Polymers at an interface: a simplified view. *Adv. Colloid Interface Sci.* 27:189–209.

Dietrich, C., and R. Tampé. 1995. Charge determination of membrane molecules in polymer-supported lipid layers. *Biochim. Biophys. Acta.* 1238:183–191.

Du, H., P. Chandaroy, and S. W. Hui. 1997. Grafted poly-(ethylene glycol) on lipid surfaces inhibits protein adsorption and cell adhesion. *Biochim. Biophys. Acta.* 1326:236–248.

Edidin, M., M. C. Zúñiga, and M. Sheetz. 1994. Truncation mutants define and locate cytoplasmic barriers to lateral mobility of membrane glycoproteins. *Proc. Natl. Acad. Sci. USA.* 91:3378–3382.

Elender, G., M. Kühner, and E. Sackmann. 1996. Functionalisation of Si/SiO_2 and glass surfaces with ultrathin dextran films and deposition of lipid bilayers. *Biosens. Bioelectron.* 11:565–577.

Evans, E., and E. Sackmann. 1988. Translational and rotational drag coefficients for a disk moving in a liquid membrane associated with a rigid structure. *J. Fluid Mech.* 194:553–561.

Fromherz, P., V. Kiessling, K. Kottig, and G. Zeck. 1999. Membrane transistor with giant lipid vesicle touching a silicon chip. *Appl. Phys. A.* 69:571–576.

Gilmanshin, R., C. E. Creutz, and L. K. Tamm. 1994. Annexin IV reduces the rate of lateral lipid diffusion and changes the fluid phase structure of the lipid bilayer when it binds to negatively charged membranes in the presence of calcium. *Biochemistry.* 33:8225–8232.

Heyse, S., T. Stora, E. Schmid, J. H. Lakey, and H. Vogel. 1998. Emerging techniques for investigating molecular interactions at lipid membranes. *Biochim. Biophys. Acta.* 137:319–338.

Hinterdorfer, P., G. Baber, and L. K. Tamm. 1994. Reconstitution of membrane fusion sites. A total internal reflection fluorescence microscopy study of influenza hemagglutinin-mediated membrane fusion. *J. Biol. Chem.* 269:20360–20368.

Holloway, P. W., and C. Buchheit. 1990. Topography of the membrane-binding domain of cytochrome b_5 in lipids by Fourier-transform infrared spectroscopy. *Biochemistry.* 29:9631–9637.

Hubbard, J. B., V. Silin, and A. L. Plant. 1998. Self assembly of hydrophobic interactions at alkanethiol monolayers: mechanism of formation of hybrid bilayer membranes. *Biophys. Chem.* 75:163–176.

Huber, R., J. Römisch, and E.-P. Paques. 1990. The crystal structure of human annexin V, an anticoagulant protein that binds to calcium and membranes. *EMBO J.* 9:3867–3874.

Isas, J. M., J.-P. Cartailler, Y. Sokolov, D. R. Patel, R. Langen, H. Luecke, J. E. Hall, and H. T. Haigler. 2000. Annexins V and XII insert into bilayers at mildly acidic pH and form ion channels. *Biochemistry.* 39:3015–3022.

Jin, H. L., B. L. Hai, and J. D. Andrade. 1995. Blood compatibility of polyethylene oxide surfaces. *Prog. Polym. Sci.* 20:1043–1079.

Johnson, S. J., T. M. Bayerl, D. C. McDermott, G. W. Adam, A. R. Rennie, R. K. Thomas, and E. Sackmann. 1991. Structure of an adsorbed dimyristoylphosphatidylcholine bilayer measured with specular reflection of neutrons. *Biophys. J.* 59:289–294.

Kalb, E., J. Engel, and L. K. Tamm. 1990. Binding of proteins to specific target sites in membranes measured by total internal reflection fluorescence spectroscopy. *Biochemistry.* 29:1607–1613.

Kalb, E., S. Frey, and L. K. Tamm. 1992. Formation of supported planar bilayers by fusion of vesicles to supported phospholipid monolayers. *Biochim. Biophys. Acta.* 1103:307–316.

Kalb, E., and L. K. Tamm. 1992. Incorporation of cytochrome b_5 into supported phospholipid bilayers by vesicle fusion to supported monolayers. *Thin Solid Films.* 210/211:763–765.

Kuhl, T. L., D. E. Leckband, D. D. Lasic, and J. N. Israelachvili. 1994. Modulation of interaction forces between bilayers exposing short-chained ethylene oxide headgroups. *Biophys. J.* 66:1479–1488.

Kuhl, T. L., J. Majewski, J. Y. Wong, S. Steinberg, D. E. Leckband, J. N. Israelachvili, and G. S. Smith. 1998. A neutron reflectivity study of polymer-modified phospholipid monolayers at the solid-solution interface: polyethylene glycol-lipids on silane-modified substrates. *Biophys. J.* 75:2352–2362.

Kühner, M., R. Tampé, and E. Sackmann. 1994. Lipid mono- and bilayer supported on polymer films: composite polymer-lipid films on solid substrates. *Biophys. J.* 67:217–226.

Ladokhin, A. S., and P. W. Holloway. 1995. Fluorescence of membrane-bound tryptophan octyl ester: a model for studying intrinsic fluorescence of protein-membrane interactions. *Biophys. J.* 69:506–517.

Ladokhin, A. S., L. Wang, A. W. Steggles, and P. W. Holloway. 206. 1991. Fluorescence study of a mutant cytochrome b_5 with a single tryptophan in the membrane-binding domain. *Biochemistry.* 30:10200–10210.

Langen, R., J. M. Isas, W. L. Hubbell, and H. T. Haigler. 1998. A transmembrane form of annexin XII detected by site-directed spin labeling. *Proc. Natl. Acad. Sci. USA.* 95:14060–14065.

Majewski, J., T. L. Kuhl, M. C. Gerstenberg, J. N. Israelachvilli, and G. S. Smith. 1997. Structure of phospholipid monolayers containing poly(ethylene glycol) lipids at the air-water interface. *J. Phys. Chem. B.* 101: 3122–3129.

Majewski, J., T. L. Kuhl, K. Kjar, M. C. Gerstenberg, J. Als-Nielsen, J. N. Israelachvilli, and G. S. Smith. 1998a. X-ray synchrotron study of packing and protrusions of polymer-lipid monolayers at the air-water interface. *J. Am. Chem. Soc.* 120:1469–1473.

Majewski, J., J. Y. Wong, C. K. Park, M. Seitz, J. N. Israelachville, and G. S. Smith. 1998b. Structural studies of polymer-cushioned lipid bilayers. *Biophys. J.* 75:2363–2367.

McConnell, H. M., T. H. Watts, R. M. Weis, and A. A. Brian. 1986. Supported planar membranes in studies of cell-cell recognition in the immune system. *Biochim. Biophys. Acta.* 864:95–106.

Poglitsch, C. L., M. T. Sumner, and N. L. Thompson. 1991. Binding of IgG to MoFcγRII purified and reconstituted into supported planar membranes as measured by total internal reflection fluorescence microscopy. *Biochemistry.* 30:6662–6671.

Prime, K. L., and G. M. Whitsides. 1991. Self-assembled organic monolayers: model systems for studying adsorption of proteins at surfaces. *Science.* 252:1164–1167.

Reviakine, I., W. Bergsma-Schutter, and A. Brisson. 1998. Growth of protein 2-D crystals on supported planar lipid bilayers imaged in situ by AFM. *J. Struct. Biol.* 121:356–361.

Rex, S., M. J. Zuckermann, M. Lafleur, and J. R. Silvius. 1998. Experimental and Monte Carlo simulation studies of the thermodynamics of polyethyleneglycol chains grafted to lipid bilayers. *Biophys. J.* 75: 2900–2914.

Sackmann, E. 1996. Supported membranes: scientific and practical applications. *Science.* 271:43–48.

Salafsky, J., J. T. Groves, and S. G. Boxer. 1996. Architecture and function of membrane proteins in supported bilayers: a study with photosynthetic reaction centers. *Biochemistry.* 35:14773–14781.

Saxton, M. J., and K. Jacobson. 1997. Single-particle tracking: applications to membrane dynamics. *Annu. Rev. Biophys. Biomol. Struct.* 26: 373–399.

Schütz, G. J., H. Schindler, and T. Schmidt. 1997. Single-molecule microscopy on model membranes reveals anomalous diffusion. *Biophys. J.* 73:1073–1080.

Seaton, B. A. 1996. Annexins: Molecular Structure to Cellular Function. Landes. Austin, TX.

Silvestro, L., and P. H. Axelsen. 1998. Infrared spectroscopy of supported lipid monolayer, bilayer, and multibilayer membranes. *Chem. Phys. Lipids.* 96:69–80.

Smith, B. A., and H. M. McConnell. 1978. Determination of molecular motion in membranes using periodic pattern photobleaching. *Proc. Natl. Acad. Sci. USA.* 75:2759–2763.

Spinke, J., J. Yang, H. Wolf, M. Lily, H. Ringsdorf, and W. Knoll. 1992. Polymer- supported bilayer on a solid substrate. *Biophys. J.* 63: 1667–1671.

Stelzle, M., G. Weismüller, and E. Sackmann. 1993. On the application of supported bilayers as receptive layers for biosensors with electrical detection. *J. Phys. Chem.* 97:2974–2981.

Stora, T., J. H. Lakey, and H. Vogel. 1999. Ion-channel gating in transmembrane receptor proteins: functional activity in tethered lipid membranes. *Angew. Chem. Int. Ed.* 38:389–392.

Tamm, L. K. 1988. Lateral diffusion and fluorescence microscope studies on a monoclonal antibody specifically bound to supported phospholipid bilayers. *Biochemistry.* 27:1450–1457.

Tamm, L. K. 1993. Total internal reflectance fluorescence microscopy. *In* Optical Microscopy: Emerging Methods and Applications. Academic Press, San Diego. 295–337.

Tamm, L. K., and E. Kalb. 1993. Microspectrofluorometry on supported planar membranes. *In* Molecular Luminescence Spectroscopy, Part 3. S.G. Schulmann, editor. John Wiley and Sons, New York. 253–305.

Tamm, L. K., and H. M. McConnell. 1985. Supported phospholipid bilayers. *Biophys. J.* 47:105–113.

Tamm, L. K., and Z. Shao. 1998. The application of AFM to biomembranes. *In* Biomembrane Structure. D. Chapman and P. Haris, editors. IOS Press, Amsterdam. 169–185.

Tamm, L. K., and S. A. Tatulian. 1997. Infrared spectroscopy of proteins and peptides in lipid bilayers. *Q. Rev. Biophys.* 30:365–429.

Thomas, R. N., and J. J. O'Malley. 1979. Surface studies on multicomponent polymer systems by x-ray photoelectron spectroscopy. Polystyrene/poly(ethylene oxide) diblock copolymers. *Macromolecules.* 12: 323–329.

Thompson, N. L., A. W. Drake, L. Chen, and W. Vanden Broek. 1997. Equilibrium, kinetics, diffusion and self-association of proteins at membrane surfaces: measurement by total internal reflection fluorescence microscopy. *Photochem. Photobiol.* 65:39–46.

Thompson, N. L., K. H. Pearce, and H. V. Hsieh. 1993. Total internal reflection fluorescence microscopy: application to substrate-supported planar membranes. *Eur. Biophys. J.* 22:367–378.

van Oudenaarden, A., and S. G. Boxer. 1999. Brownian ratchets: molecular separations in lipid bilayers supported on patterned arrays. *Science.* 285:1046–1048.

Vaz, W. L. C., F. Goodsaid-Zalduondo, and K. Jacobson. 1984. Lateral diffusion of lipids and proteins in bilayer membranes. *FEBS Lett.* 174: 199–207.

Vergères, G., J. Ramsden, and L. Waskell. 1995. The carboxyl terminus of the membrane-binding domain of cytochrome b_5 spans the bilayer of the endoplasmic reticulum. *J. Biol. Chem.* 270:3414–3422.

Voges, D., R. Berendes, A. Burger, P. Demange, W. Baumeister, and R. Huber. 1994. Three-dimensional structure of membrane-bound annexin V. A correlative electron microscopy-x-ray crystallography study. *J. Mol. Biol.* 238:199–213.

Wenzl, P., M. Fringeli, J. Goette, and U. P. Fringeli. 1994. Supported phospholipid bilayers prepared by the "LB/vesicle method": a Fourier transform infrared attenuated total reflection spectroscopic study on structure and stability. *Langmuir.* 10:4253–4264.

Woodle, M. C., and D. D. Lasic. 1992. Sterically stabilized liposomes. *Biochim. Biophys. Acta.* 1113:171–199.

Wong, J. Y., J. Majewski, M. Steitz, C. K. Park, J. N. Israelachvili, and G. S. Smith. 1999a. Polymer-cushioned bilayers. I. Structural study of various preparation methods using neutron reflectometry. *Biophys. J.* 77:1445–1457.

Wong, J. Y., C. K. Park, M. Steitz, and J. N. Israelachvili. 1999b. Polymer-cushioned bilayers. II. An investigation of interaction forces and fusion using the surface forces apparatus. *Biophys. J.* 77:1458–1468.